JOURNAL OF Applied Polymer SCIENCE

Effect of Ultrasonic Irradiation on the Microstructure and the Electric Property of PP/CPP/MWNT Composites

Lin Yang,[1,2] Zhiye Zhang,[1] Xinlong Wang,[1] Jinyao Chen,[2] Huilin Li[2]
[1]College of Chemical Engineering of Sichuan University, Chengdu, Sichuan 610065, China
[2]State Key Laboratory of Polymer Materials Engineering, Polymer Research Institute of Sichuan University, Chengdu, Sichuan 610065, China
Correspondence to: H. Li (E-mail: nic7703@scu.edu.cn)

ABSTRACT: Poly(propylene) (PP)/chlorinated PP (CPP)/multiwalled carbon nanotube (MWNT) composites are prepared via melting blend with a MWNT masterbatch obtained by a solution process under ultrasonic irradiation. The effects of ultrasonic irradiation on the microstructure and the electric properties of the PP/CPP/MWNT composites are systematically investigated through a combination of scanning electron microscopy (SEM), transmission electron microscopy (TEM), wide-angle X-ray diffraction (WAXD), and rheological measurements. Ultrasonic irradiation can remarkably decrease the volume resistivity of the PP/CPP/MWNT composites. The results of SEM and TEM show that the ultrasonic irradiation is beneficial to the dispersion of MWNTs in the PP/CPP/MWNT composites and the exfoliation of the MWNT agglomerates. When the MWNT content is more than 3.0%, ultrasonic irradiation can evidently increase the percent crystallinity of the PP/CPP/MWNT composites. The introduction of ultrasonic irradiation can increase the elastic modulus (G'), viscous modulus (G''), and complex viscosity (η^*) of the PP/CPP/MWNT composites at low frequency. Ultrasonic irradiation is also shown to improve the interfacial adhesion of MWNT and the interaction between the PP matrix and MWNT. © 2012 Wiley Periodicals, Inc. J. Appl. Polym. Sci. 000: 000–000, 2012

KEYWORDS: composites; poly(propylene); structure

Received 13 April 2011; accepted 3 July 2012; published online
DOI: 10.1002/app.38297

INTRODUCTION

The favorable mechanical properties and electrical conductivity of carbon nanotubes (CNTs), including single-walled CNTs and multiwalled CNTs (MWNTs), have made them very attractive for use in nanocomposites endowed with good electrical conductivity or superior reinforcing capability.[1–7] Low concentration of CNT added in polymers can enhance the mechanical[8–14] and electrical properties of the composites.[15–17] The nanotube composites with extraordinary electrical properties can be used for applications in electrostatic dissipation, electromagnetic interference shielding, radiofrequency interference shielding, and so forth.[18]

The dispersion of CNTs in composites plays a prominent role in the decision of the mechanical and electrical properties of the polymer/CNT composites. Homogeneous distribution of CNTs usually leads to an obvious improvement in the mechanical and electrical properties of the resulting composites. However, because of the van der Waals attraction between nanotubes, CNTs may exhibit agglomerate phenomenon and poor interfacial adhesion, and therefore, it is difficult to disperse CNTs in polymer matrix uniformly.[19,20] The agglomeration of CNTs reduces the surface area of the CNT and interrupts the formation of the conductive network, which is essential to improve the electrical and mechanical properties.

Usually, many methods such as end-group functionalization,[21–25] use of ionic surfactants,[26] shear mixing,[27,28] plasma coating,[29] and ultrasonic irradiation[30–32] have been used to improve the dispersion of CNTs. Although these methods can improve the dispersion of CNTs to some extent, there are some disadvantages. For example, CNTs can be grafted with some functional groups to facilitate better dispersion of CNTs in polymer matrix. However, this method can introduce some defects in CNTs and degrade their mechanical properties.[33] Ultrasonic irradiation is not suitable for mass production of composite materials. Solution processing has been a commonly used method in fabrication of the well-dispersed CNT composites; however, it is hard to achieve homogeneous dispersion because CNT is insoluble and bundled.[18] Acid treatment of CNTs is a well-known technique that can enhance the purity of CNTs, generate functional groups, and facilitate good dispersion of CNTs. However, this

© 2012 Wiley Periodicals, Inc.

method is complicated and can also generate a tremendous amount of waste acid.

Ultrasound was used because it has the functions of dispersion, crushing, activation, and initiation. Ultrasonic cavitations can generate local high temperature ~ 5000 K, local high pressure ~ 500 atm, and heating and cooling rate greater than 10^9 K/s, a very rigorous physicochemical environment for chemical reactions.[34,35] This study is going to take advantages of the dispersion, crushing, activation, and initiation of ultrasonic irradiation to disperse MWNT in the MWNT masterbatch, which is prepared in solution processing under the ultrasonic irradiation. In this work, the industrial-grade MWNT is acted as conductive filler, which is low in price and without any aggressive chemical treatment, purification, or modification. The poly(propylene) (PP)/chlorinated PP (CPP)/MWNT composites are prepared in the masterbatch process, which is one of the simplest and most economical methods in the processing of CNT composites. The effect of ultrasonic irradiation on the microstructure and the electric property of the PP/CPP/MWNT composites are systematically investigated through combination of scanning electron microscopy (SEM), wide-angle X-ray diffraction (WAXD), rheological measurements, and transmission electron microscopy (TEM).

EXPERIMENTAL

Materials

PP (PPH-XD-045, white powder, isotactic index = 96%, melt flow index = 3.5 g/10 min, apparent density = 0.43 g/mL, tensile yield strength = 31.5 MPa) is supplied by PetroChina (Lanzhou, China).

CPP was supplied by Sichuan Weiye Chemicals (Chengdu, China). Its chlorine content is about 31% (wt), and its color is light yellow. The viscosity of 20% (wt) of CPP in toluene solution is about 700 mPa s at 25°C.

MWNT is of industrial grade and was supplied by Chengdu Organic Chemicals (Chengdu, China). Its electrical conductivity is about 100 S/cm, its diameter is 20–40 nm, and its purity is larger than 90%.

Xylenes are analytical reagent and were supplied by Kelong Chemicals (Chengdu, China).

Preparation of Composites

Preparation of the MWNT Masterbatch. The first method: 500 mL of xylene, 10 g of CPP, and 10 g of PP were placed into a 750-mL three-necked flask equipped with a condenser under stirring for 2 h at 120°C, and then 5 g of MWNT was added in the flask under stirring for 2 h at 120°C. Finally, xylene was recovered by distillation, and the MWNT masterbatch was dried in vacuum at 50°C.

The second method: There was only one difference between the first method and the second method. The difference lied in that quantitative MWNT was added in the flask under ultrasonic irradiation for 0.5 h. The ultrasonic frequency was 20 kHz, and the power was 150 W.

The third method: The only one difference between the second method and the third method is that there is no CPP in the MWNT masterbatch.

Table I. Composition of PP/CPP/MWNT Composites (in wt %)

Sample code	MWNT (%)	MWNT masterbatch (%)	PP (%)	Volume resistivity (Ω cm^3)
PP/CPP/MWNT-N 0.5	0.5	2.5	97.5	1.38×10^{14}
PP/CPP/MWNT-N 1.0	1.0	5.0	95.0	1.22×10^{14}
PP/CPP/MWNT-N 2.0	2.0	10.0	90.0	1.19×10^{14}
PP/CPP/MWNT-N 3.0	3.0	15.0	85.0	1.07×10^{14}
PP/CPP/MWNT-N 5.0	5.0	25.0	75.0	1.04×10^{14}
PP/CPP/MWNT-U 0.5	0.5	2.5	97.5	1.27×10^{14}
PP/CPP/MWNT-U 1.0	1.0	5.0	95.0	8.24×10^{13}
PP/CPP/MWNT-U 2.0	2.0	10.0	90.0	8.60×10^{13}
PP/CPP/MWNT-U 3.0	3.0	15.0	85.0	4.86×10^{12}
PP/CPP/MWNT-U 5.0	5.0	25.0	75.0	2.97×10^{9}
PP/MWNT-U 1.0	1.0	5.0	95.0	1.06×10^{14}
PP/MWNT-U 3.0	3.0	15.0	85.0	8.49×10^{13}
PP/MWNT-U 5.0	5.0	25.0	75.0	4.59×10^{11}

Preparation of PP/CPP/MWNT Composites. The composites of PP/MWNT-U and PP/CPP/MWNT with different MWNT masterbatch contents were prepared on a two-roll mill and then molded into 1-mm plates. Compression molding was performed in the following conditions[36]: preheated at 180°C for 5 min at 0.5 MPa, compressed for 10 min at 13 MPa at 180°C, and then cooled to ambient temperature with the cooling rate 30°C/min in the mold at 13 MPa. The composite components and their sample codes are listed in Table I.

In Table I, three types of MWNT masterbatch are given. The samples with the code of PP/CPP/MWNT-N were prepared in the MWNT masterbatch without ultrasonic irradiation. Other samples with the code of PP/CPP/MWNT-U were prepared in the MWNT masterbatch with ultrasonic irradiation. The samples with code of PP/MWNT-U were prepared in the MWNT masterbatch without CPP.

Measurement of the Volume Conductivity

Specimens with the dimensions of 80 × 80 × 1 mm^3 for the test of volume resistivity were got from the 1-mm plates. The volume resistivity of the PP/CPP/MWNT composites was measured in high-resistance meter (ZC46A) produced by Shanghai precision Scientific Instrument (China). The result of each sample is average of four measurements.[36]

Scanning Electron Microscopy

The morphology of the PP/CPP/MWNT composites was observed in a JSM 5900 LV SEM. The specimens are prepared by brittle fracturing under liquid nitrogen and then sputtered with a very thin gold layer.

TEM Measurement

TEM measurement was performed on an H-7100 (Japan) field emission gun TEM operated at 100 kV. TEM samples were prepared on lacey carbon-coated 300-mesh copper grids. Ultrathin sections (about 100 nm) of sample were cut from the rectangular blocks of PP/CPP/MWNT composites by an ultramicrotome (Reichert Ultracut).

Rheological Measurement

Rheological experiments in dynamic frequency sweep mode with parallel plates geometry (25 mm in diameter) were

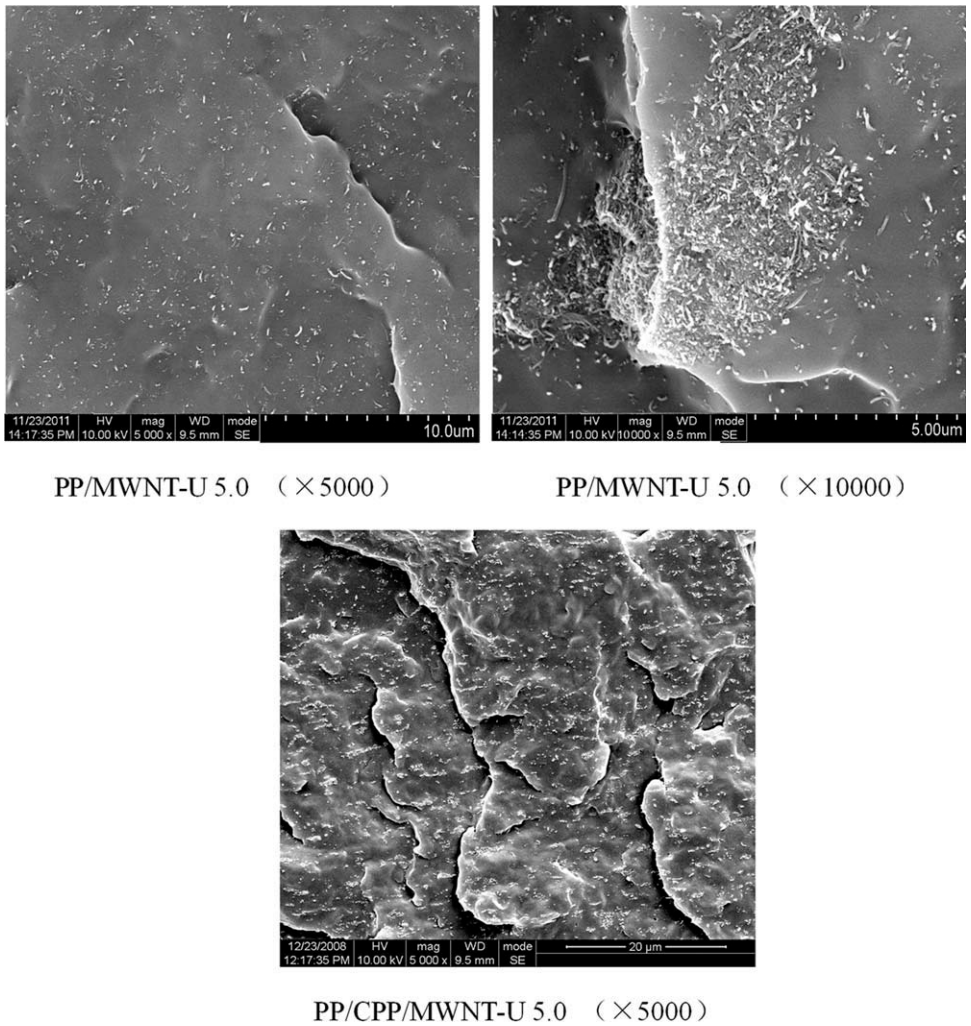

Figure 1. SEM micrographs of (a and b) PP/MWNT-U 5.0 (a: ×5000; b: ×10,000) and (c) PP/CPP/MWNT-U 5.0 composites (c: ×5000).

performed using a Bohlin Genemi 200HR rheometer (UK). Isothermal dynamic frequency sweep (0.01–100 rad/s) was performed at a given strain ($\gamma = 1\%$) in the linear viscoelastic regime at 185°C to investigate the dynamic mechanical properties of the samples.

Wide-Angle X-Ray Diffraction

A DX-2500 SSC diffractometer (made in China) was used to investigate WAXD. Cu Kα radiation was used at 40 kV and 25 mA. The crystallite size was estimated for planes of PP by using the Scherrer equation:

$$D = K\lambda/(\beta\cos\theta),$$

where D is the crystallite size in the direction perpendicular to the plane, β is the full width at half maximum, $\lambda = 0.154$ nm is the wavelength, and θ is the Bragg angle. In this study, the value 0.89 was tentatively used for K.[36,37]

Differential Scanning Calorimetry

Differential scanning calorimetry (DSC) analyses were performed on NETZSCH DSC 204. The samples were heated under nitrogen atmosphere from 40 to 200°C at a rate of 10°C/min.

RESULTS AND DISCUSSION

Effect of CPP on the Volume Resistivity and Dispersion of MWNTs in PP/CPP/MWNT Composites

In previous studies,[36,38] the microstructure and the electric properties of the PP/CPP/polyaniline (PANI) composites have been investigated, and it is shown that CPP plays a prominent role to determine the electrical properties of composite and the dispersion of PANI. The results of the measurement of the volume resistivity show (in Table I) that, when compared with PP/CPP/MWNT-U composites, the volume resistivity of PP/MWNT-U composites is much higher. The volume resistivity of PP/CPP/MWNT-U 5.0 is two orders of magnitudes lower than that of PP/MWNT-U 5.0. The introduction of CPP decreases the volume resistivity of PP/CPP/MWNT composites, which may suggest that CPP is beneficial to the dispersion of MWNTs in the PP/CPP/MWNT composites.

Figure 1 shows the SEM micrographs of PP/MWNT-U 5.0 and PP/CPP/MWNT-U 5.0 composites. When compared with the SEM micrographs of PP/MWNT-U 5.0, the dispersion of MWNTs is more uniform in the PP/CPP/MWNT-U 5.0. In the SEM micrographs of PP/MWNT-U 5.0 (×10,000), there is only

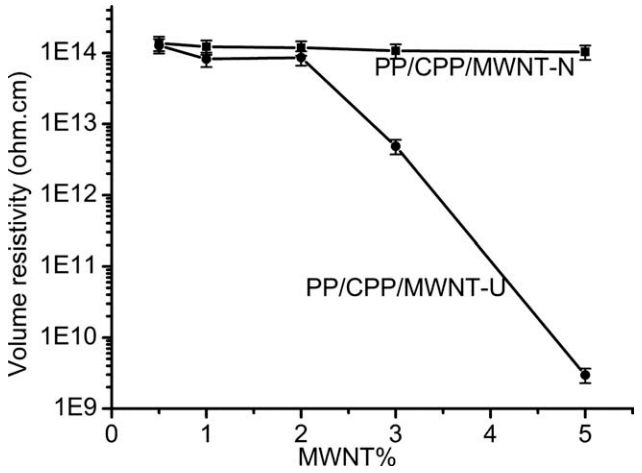

Figure 2. The relationship between the volume resistivity and the MWNT content.

a big MWNT agglomerate. However, such big MWNT agglomerate cannot be searched in PP/CPP/MWNT-U 5.0, which suggests that the addition of CPP can improve the dispersion of MWNTs in the PP/CPP/MWNT composites.

From the above analysis, it is observed that the introduction of CPP is beneficial to improve the dispersion of MWNTs in the PP/CPP/MWNT composites and to decrease the volume resistivity of PP/CPP/MWNT composites.

Effect of Ultrasonic Irradiation on the Volume Resistivity of the PP/CPP/MWNT Composites

Figure 2 shows the volume resistivity of two types of PP/CPP/MWNT composites changed with the MWNT content, and the variation trend is obviously different. The volume resistivity of PP/CPP/MWNT-U composites is much lower than that of PP/CPP/MWNT-N composites. For example, in the condition of same MWNT content, the volume resistivity of PP/CPP/MWNT-U 3.0 is two orders of magnitudes lower than that of PP/CPP/MWNT-N 3.0. For the PP/CPP/MWNT-N composites prepared in the MWNT masterbatch without ultrasonic irradiation, the volume resistivity decreases with increasing MWNT content; however, the decrement is very small. However, for the PP/CPP/MWNT-U composites prepared in the MWNT masterbatch with ultrasonic irradiation, the volume resistivity remarkably decreases with increasing MWNT content. For example, the volume resistivity of PP/CPP/MWNT-U 5.0 is four orders of magnitudes lower than that of PP/CPP/MWNT-U 1.0. The reason for the above phenomenon may be that the ultrasonic irradiation can improve the dispersion of MWNTs in PP/CPP/MWNT composites and facilitate better formation of the conductive network, which is essential to decrease the volume resistivity.

SEM Analysis of the PP/CPP/MWNT Composites

Figure 3 shows the SEM micrographs of PP/CPP/MWNT-N composites with the magnification of 5000 times. In Figures 3 and 4, the white stripe is the fracture trace of the specimens; the white particles and agglomerates are the MWNT, which is proved in Figure 5. When the MWNT content is low, the dispersion of MWNTs in the composites is poor, and there are a little MWNT agglomerates in the SEM micrographs. With the increasing MWNT content, the dispersion of MWNTs is not improved, and the size of the MWNT agglomerates increases. As shown in the SEM micrograph of PP/CPP/MWNT-N 5.0, there are several big MWNT agglomerates in the composite. Therefore, in the PP/CPP/MWNT-N composites, not all the increasing MWNTs participate in the formation of the conductive network; most of the MWNTs form the MWNT agglomerates. Hence, with the increasing MWNT content, the decrement of the volume resistivity is very small.

Figure 4 shows the SEM micrographs of PP/CPP/MWNT-U composites with the magnification of 5000 times. In all the SEM micrographs of PP/CPP/MWNT-U composites, there is no prominent agglomerate phenomenon, and the dispersion of MWNTs in the matrix is homogeneous. When comparing Figure 4 with Figure 3, the dispersion of MWNTs in the PP/CPP/MWNT-U composites is much better than that in the PP/CPP/MWNT-N composites. Figure 4 also shows that when the MWNT content is low, the number of MWNT particle is exiguous, and it is very difficult to form a perfect conductive network. Therefore, its volume resistivity is high. With the increasing MWNT content, the number of MWNT particles dramatically increase, and the continuity of MWNT particles is improved. For instance, when compared with PP/CPP/MWNT-U 3.0, the number of MWNT particles is much higher in PP/CPP/MWNT-U 5.0, its SEM micrograph is full of MWNT particles, and it is easy to form a perfect conductive network. Hence, the volume resistivity of PP/CPP/MWNT-U 5.0 is three orders of magnitudes lower than that of PP/CPP/MWNT-U 3.0.

To further investigate the effect of ultrasonic irradiation on the dispersion of MWNTs, the SEM micrographs of PP/CPP/MWNT composites are digitally analyzed. As seen in Figure 3, there is prominent agglomerate phenomenon in PP/CPP/MWNT-N 2.0, 3.0, and 5.0, and even some SEM micrographs are full of big MWNT agglomerates. This phenomenon is not beneficial to digitally analyze the SEM micrograph. Therefore, SEM micrographs of PP/CPP/MWNT-N 0.5 and 1.0 and PP/CPP/MWNT-U 0.5 and 1.0 are chosen to be digitally analyzed. If the intensity of white is defined 255 and that of black is defined 0, and then the range of the color intensity is defined from 0 to 255 in the SEM image, SEM micrographs can be digitally analyzed. The area of the range of the color intensity can be statistical. Figure 5 shows the SEM micrographs of PP/CPP/MWNT-N 0.5 composite with the different magnification. As seen in Figure 5, the white stripe is the fracture trace of the specimens; the white particles and agglomerates are the MWNT. Hence, to be statistically convenient, the white stripes are converted into black; the range of intensity 235–255 may be regarded as the MWNT. The number of MWNT conglomeration and the area of the maximal agglomerate in SEM micrographs are statistically analyzed using the software Sigma Scan. The statistical value of each sample is average of three micrographs, which is listed in Table II.

Table II shows that the area of the maximal agglomerate increases with the increasing MWNT content in the PP/CPP/MWNT composites. However, the increment of the maximal agglomerate's

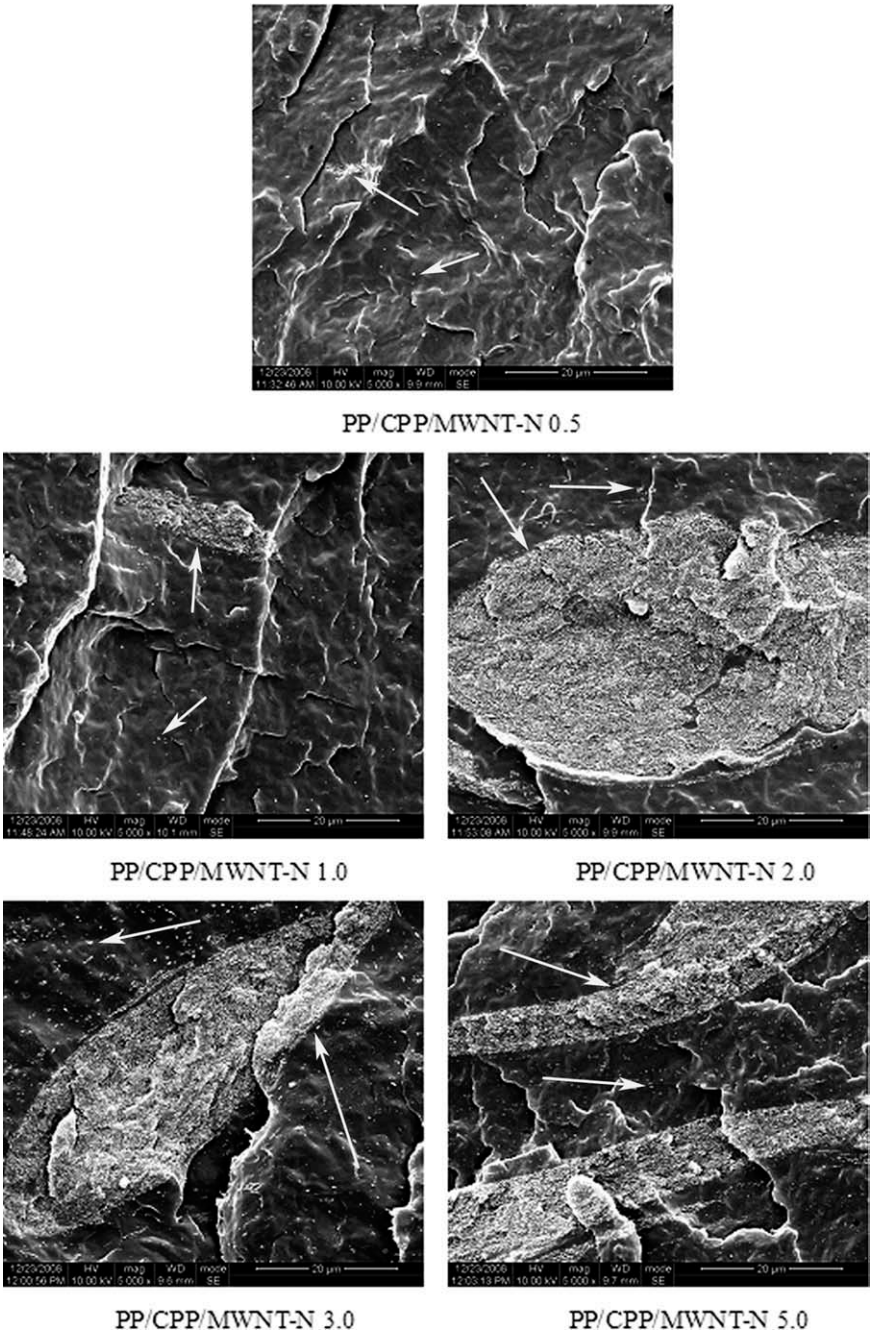

Figure 3. SEM micrographs of PP/CPP/MWNT-N composites (×5000): (a) PP/CPP/MWNT-N 0.5; (b) PP/CPP/MWNT-N 1.0; (c) PP/CPP/MWNT-N 2.0; (d) PP/CPP/MWNT-N 3.0; and (e) PP/CPP/MWNT-N 5.0.

area in the PP/CPP/MWNT-U composites is much lower than that in the PP/CPP/MWNT-N composites. The maximal agglomerate's area in PP/CPP/MWNT-N 1.0 is three times wider than that in PP/CPP/MWNT-N 0.5. The maximal agglomerate's area in PP/CPP/MWNT-U 1.0 is two times as wide as that in PP/CPP/MWNT-U 0.5. The number of MWNT particles increases with the increasing MWNT content in the PP/CPP/MWNT composites. However, the increment of the number in the PP/CPP/MWNT-U composites is much higher than that in the PP/CPP/MWNT-N composites. From the above analysis, it is observed that the ultrasonic irradiation is beneficial to the dispersion of MWNTs in the PP/CPP/MWNT composites.

In addition, the number of MWNT particles in SEM micrographs is statistically analyzed. In the graphical analysis process, it is found that the area of the least MWNT particle of every sample is 0.00336 μm^2, and the other particle's area is integral multiple as wide as the least area. All the MWNT particles are divided into two groups. One is the big conglomeration and its area exceeds 0.0504 μm^2; another is the little particle and its area does not exceed 0.0504 μm^2.

Applied Polymer SCIENCE

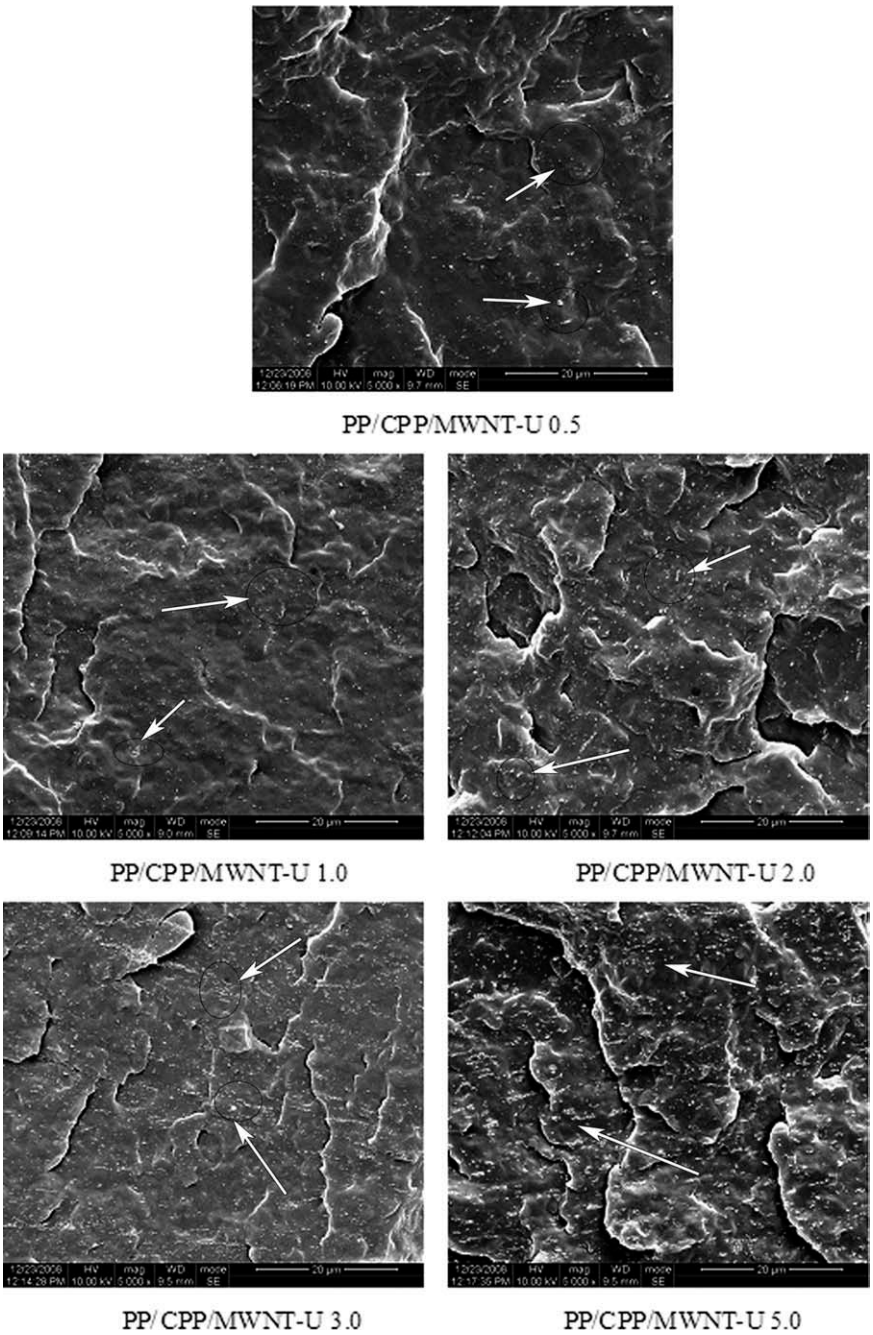

Figure 4. SEM micrographs of PP/CPP/MWNT-U composites (×5000): (a) PP/CPP/MWNT-U 0.5; (b) PP/CPP/MWNT-U 1.0; (c) PP/CPP/MWNT-U 2.0; (d) PP/CPP/MWNT-U 3.0; and (e) PP/CPP/MWNT-U 5.0.

Figure 6 shows the number of little MWNT particles whose area does not exceed 0.0504 μm^2 in PP/CPP/MWNT-N 0.5 and 1.0 and PP/CPP/MWNT-U 0.5 and 1.0. The number of little MWNT particles in PP/CPP/MWNT-N 1.0 is subequal to that in PP/CPP/MWNT-N 0.5. However, the number of little MWNT particles in PP/CPP/MWNT-U 1.0 is much more than that in PP/CPP/MWNT-U 0.5. When compared with the PP/CPP/MWNT-N composites, the number of little MWNT particles can be markedly increased with the increasing MWNT content under the ultrasonic irradiation. Hence, the ultrasonic irradiation can make the MWNT agglomerates to facilitate exfoliation.

TEM Analysis

Figure 7 shows TEM micrographs of PP/CPP/MWNT-N 5.0 and PP/CPP/MWNT-U 5.0 composites and the prominent effect of ultrasonic irradiation on the dispersion of MWNTs in the PP/CPP/MWNT composites. There are only several tremendous MWNT agglomerates in the TEM micrograph of PP/CPP/MWNT-N 5.0 (1 μm). Apparently, the presence of MWNT agglomerates reduces the surface area of the MWNT and interrupts the formation of the conductive network. However, there are many little MWNT particles in the TEM micrograph of PP/CPP/MWNT-U 5.0 (1 μm), which is facilitated to the better formation of the conductive

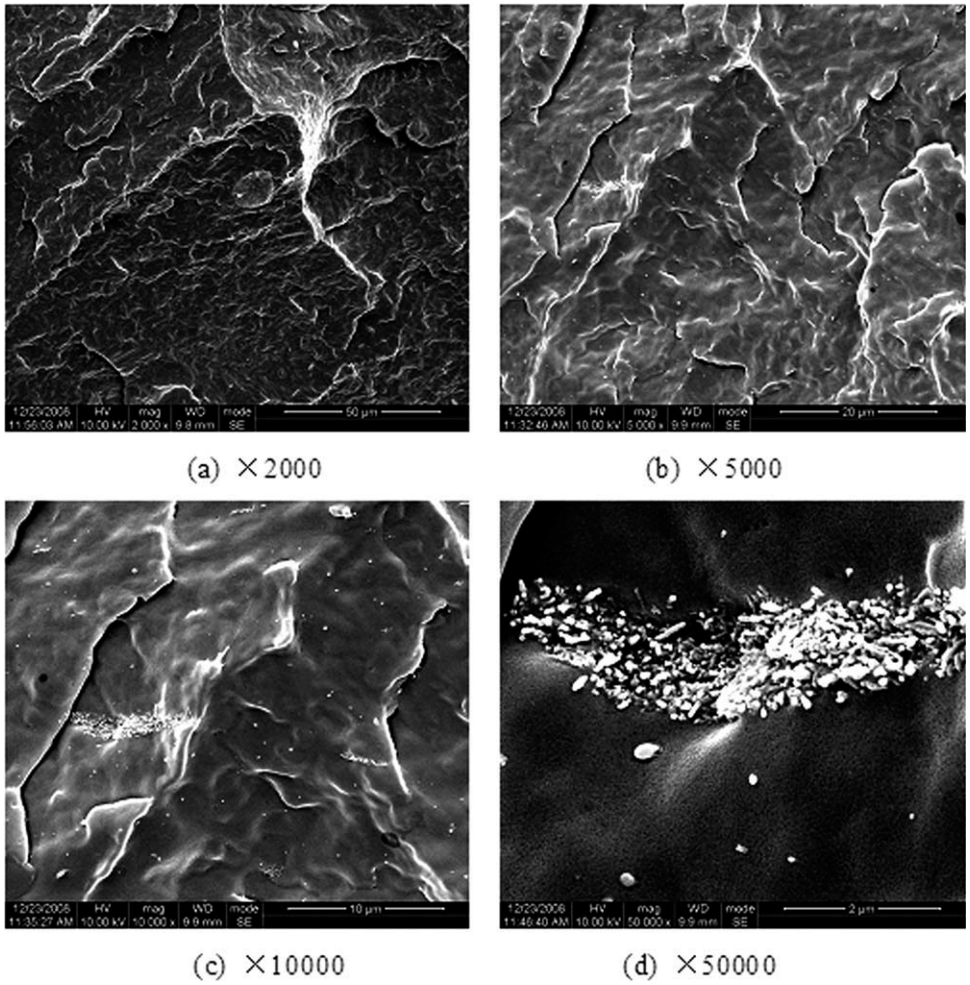

Figure 5. SEM micrographs of PP/CPP/MWNT-N 0.5 composite with different magnification: (a) ×2000; (b) ×5000; (c) ×10,000; and (d) ×50,000.

network and results in the remarkable decrease of the volume resistivity of PP/CPP/MWNT-U 5.0. In the TEM micrograph of PP/CPP/MWNT-N 5.0 (100 nm), MWNTs are entwisted each other in a big MWNT agglomerate. However, in the TEM micrograph of PP/CPP/MWNT-U 5.0 (100 nm), the entwisted phenomenon is scarce, and most of the MWNTs are exfoliated and dispersed in PP matrix uniformly. When compared with the TEM micrograph of PP/CPP/MWNT-N 5.0 (100 nm) and PP/CPP/MWNT-U 5.0 (100 nm), the effect of the ultrasonic irradiation on the length of MWNT is not outstanding. Thus, it can be seen that the ultrasonic irradiation can make the MWNT agglomerates to facilitate exfoliation and to improve the dispersion of MWNTs in the PP/CPP/MWNT composites.

Table II. Statistical Results of the SEM Photograph (×5000)

Sample code	Number of MWNT conglomeration	Maximum area (μm^2)
PP/CPP/MWNT-N 0.5	3407	4.614
PP/CPP/MWNT-N 1.0	3635	18.45
PP/CPP/MWNT-U 0.5	3786	2.268
PP/CPP/MWNT-U 1.0	5900	4.497

Dynamic Rheological Behavior Analysis

Figures 8–10 show the relationship between the frequency and G', G'', and η^*, respectively, at 185°C. At low frequency, the G', G'', and η^* of PP/CPP/MWNT-N 5.0 and PP/CPP/MWNT-U

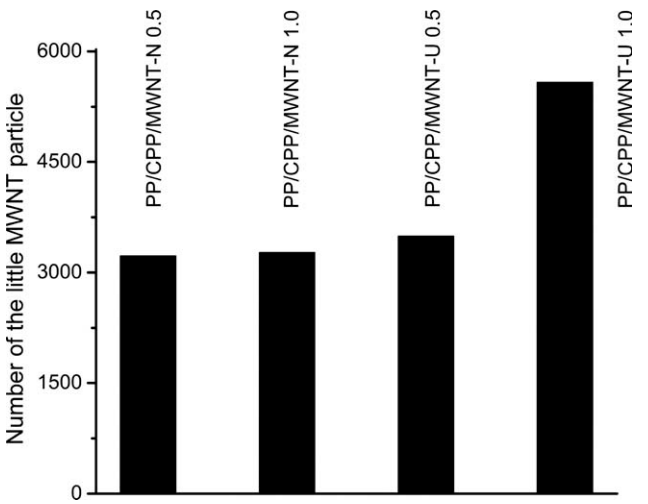

Figure 6. The number of MWNT particles in the PP/CPP/MWNT composites.

Applied Polymer SCIENCE

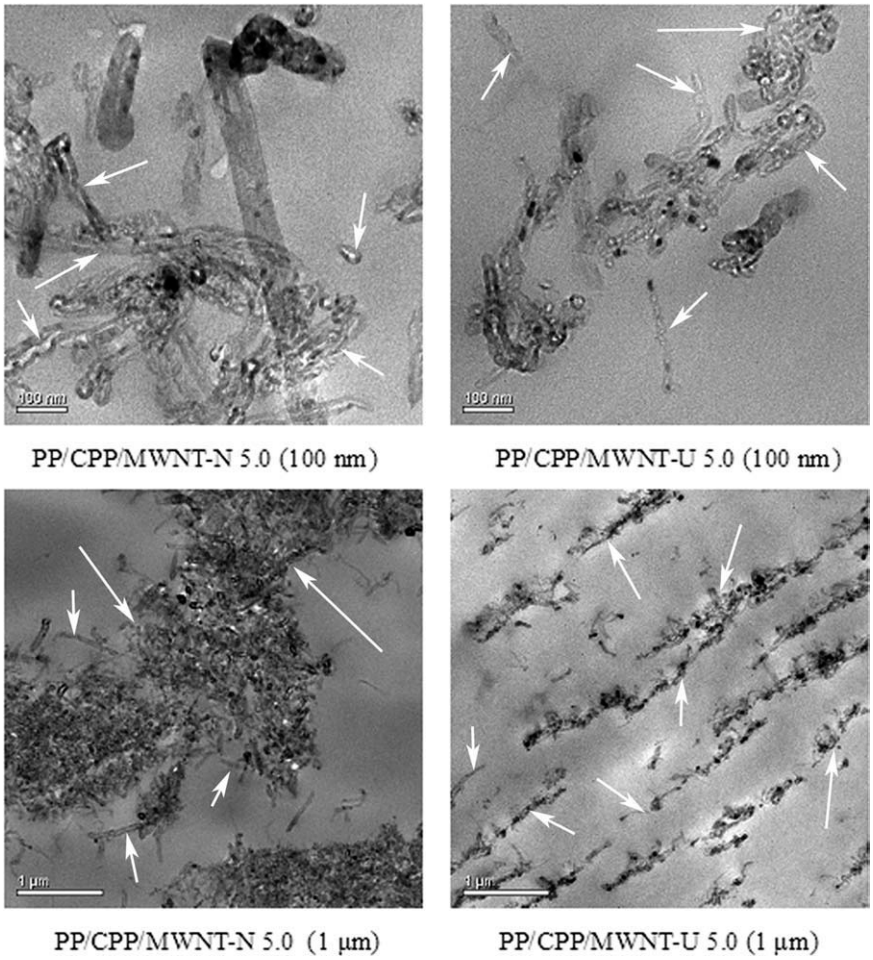

Figure 7. TEM micrographs of (a and b) PP/CPP/MWNT-N 5.0 (a: 100 nm; b: 1 μm) and (c and d) PP/CPP/MWNT-U 5.0 composites (c: 100 nm; d: 1 μm).

5.0 are higher than that of pure PP. The reason for this phenomenon may be that the molecular chains of PP are restricted by MWNTs in the PP/CPP/MWNT composites, which makes the G', G'', and η^* of the PP/CPP/MWNT composites increase at low frequency. The G', G'', and η^* of PP/CPP/MWNT-U 5.0 are higher than that of PP/CPP/MWNT-N 5.0 at all the ranges of frequency. Especially, at low frequency, the G', G'', and η^* of PP/CPP/MWNT-U 5.0 enhance prominently. It follows that the ultrasonic irradiation is beneficial to improve the interfacial

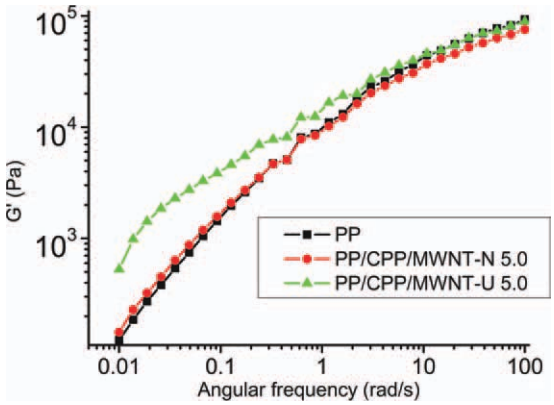

Figure 8. Effect of ultrasonic irradiation on elastic modulus of composites. [Color figure can be viewed in the online issue, which is available at wileyonlinelibrary.com.]

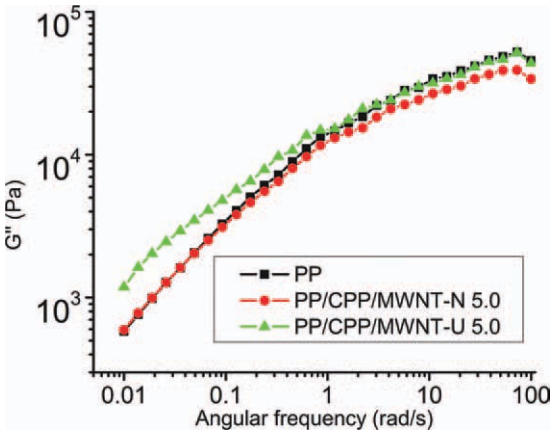

Figure 9. Effect of ultrasonic irradiation on viscous modulus of composites. [Color figure can be viewed in the online issue, which is available at wileyonlinelibrary.com.]

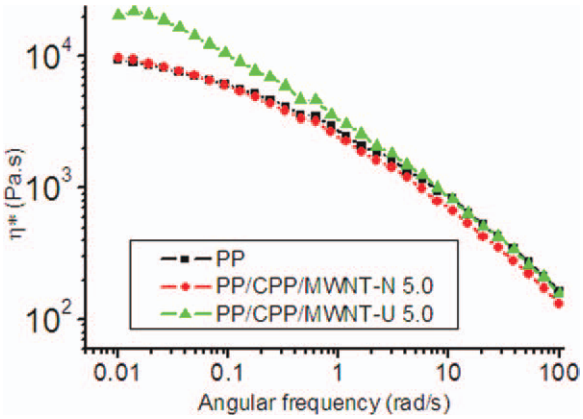

Figure 10. Effect of ultrasonic irradiation on complex viscosity of composites. [Color figure can be viewed in the online issue, which is available at wileyonlinelibrary.com.]

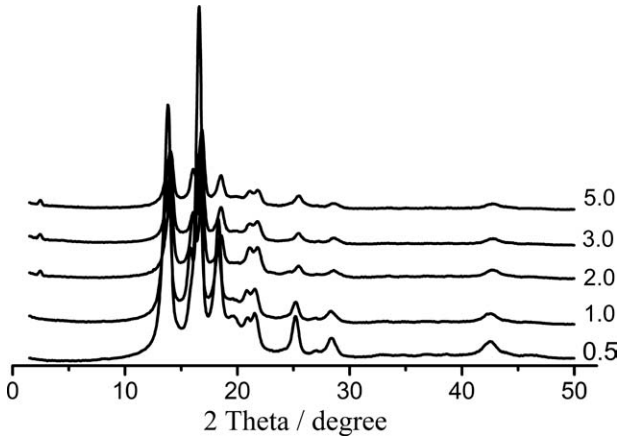

Figure 11. WAXD patterns of the PP/CPP/MWNT-N composites.

adhesion of MWNT and the interaction between PP matrix and MWNT.

WAXD Study

Figures 11 and 12 show the WAXD patterns of the PP/CPP/MWNT composites prepared without and with ultrasonic irradiation, respectively. The crystalline peaks at about 14°, 17°, 18.5°, 21°, and 21.8° are attributed to α-crystal, and the crystalline peak at about 16° is attributed to β-crystal.[39] To quantify the influence of the ultrasonic irradiation on the crystal structure of PP in the composites, WAXD curves in Figures 11 and 12 were fitted using the profile-fitting program JADE6.5. The crystal size corresponding to peaks and the percent crystallinity of the composites were calculated according to the previous study.[36] The profile-fitting results of the WAXD curves are listed in Tables III and IV.

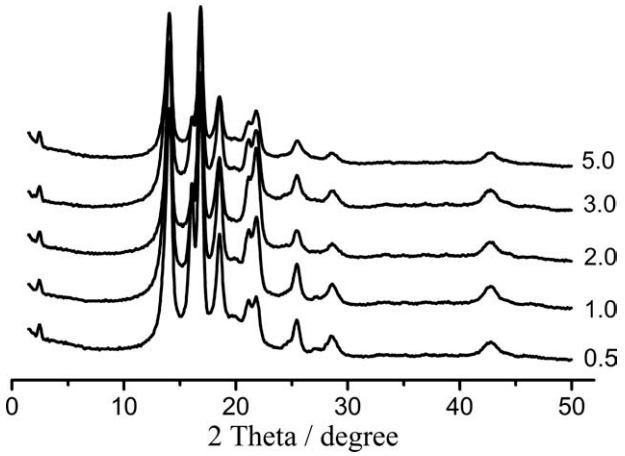

Figure 12. WAXD patterns of the PP/CPP/MWNT-U composites.

When comparing Table III with Table IV, it is found that the effect of the ultrasonic irradiation on the structural parameters of crystal is small; however, the effect on the crystallinity index (X_C) is prominent. The X_C of the PP/CPP/MWNT-N composites is slightly influenced by the MWNT content. However, the X_C of the PP/CPP/MWNT-U composites increases with the increasing MWNT content. The trend of X_C changed with the MWNT content is analogous to that of the volume resistivity changed with the MWNT content. When the MWNT content exceeds 3.0%, the effect of the ultrasonic irradiation on the X_C is obvious. For example, the X_C of PP/CPP/MWNT-U 5.0 is much higher than that of PP/CPP/MWNT-U 3.0 and PP/CPP/MWNT-N 5.0.

DSC Analysis

DSC patterns of the PP/CPP/MWNT-N and PP/CPP/MWNT-U composites are depicted in Figures 13 and 14, respectively.

Table III. Structural Parameters for the PP/CPP/MWNT-N Composites by Means of WAXD

		d (Å)				XS (Å)			
Sample code	X_C (%)	A_{110}	B_{300}	A_{040}	A_{130}	A_{110}	B_{300}	A_{040}	A_{130}
PP/CPP/MWNT-N 0.5	43	6.39		5.32	4.84	116		154	138
PP/CPP/MWNT-N 1.0	44	6.40	5.61	5.33	4.84	117	134	166	141
PP/CPP/MWNT-N 2.0	43	6.28	5.52	5.26	4.78	121	166	161	125
PP/CPP/MWNT-N 3.0	43	6.28	5.52	5.26	4.79	118	182	160	137
PP/CPP/MWNT-N 5.0	44	6.28	5.52	5.26	4.79	113	158	157	129

X_C: crystallinity index; d, interplanar distance; XS, size of crystallite corresponding to appointed peak; A_{110}, A_{040}, and A_{130}: the 110, 040, and 130 crystal face of α-crystal; B_{300}: the 300 crystal face of β-crystal.

Table IV. Structural Parameters for the PP/CPP/MWNT-U Composites by Means of WAXD

		d (Å)				XS (Å)			
Sample code	X_C (%)	A_{110}	B_{300}	A_{040}	A_{130}	A_{110}	B_{300}	A_{040}	A_{130}
PP/CPP/MWNT-U 0.5	44	6.28	5.52	5.25	4.79	118	186	164	145
PP/CPP/MWNT-U 1.0	45	6.29	5.52	5.26	4.78	114	136	156	147
PP/CPP/MWNT-U 2.0	45	6.29		5.24	4.79	105		147	120
PP/CPP/MWNT-U 3.0	50	6.29	5.52	5.26	4.78	110	116	157	136
PP/CPP/MWNT-U 5.0	65	6.29	5.51	5.26	4.79	118	142	149	111

From the DSC curves, the crystallinity of PP can be calculated, and it is listed in Table V.

Table V shows that the X_C of the PP/CPP/MWNT-N composites is slightly influenced by the MWNT content. However, the X_C of the PP/CPP/MWNT-U composites increases with the increasing MWNT content. Generally, the effect of the ultrasonic irradiation on the crystallinity of PP is prominent. When the MWNT content is larger than 2%, the ultrasonic irradiation can improve the crystallinity of PP. The trend of X_C changed with the MWNT content is analogous to that of the volume resistivity changed with the MWNT content. The results on the crystallinity of PP obtained from DSC are similar to that obtained from WAXD.

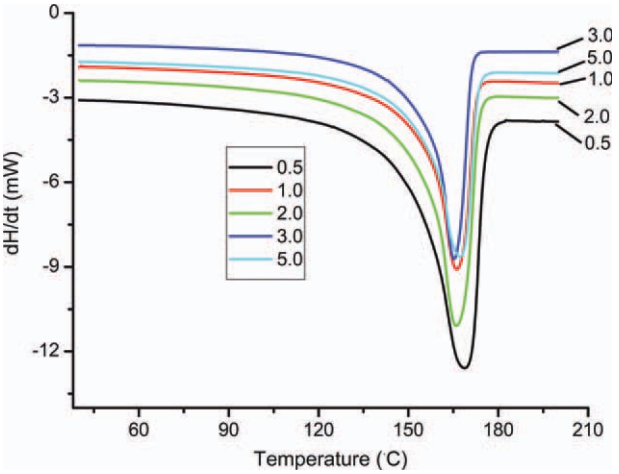

Figure 13. DSC patterns of the PP/CPP/MWNT-N composites. [Color figure can be viewed in the online issue, which is available at wileyonlinelibrary.com.]

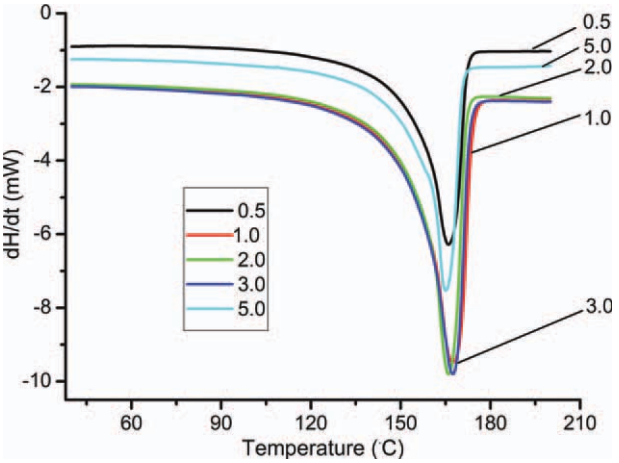

Figure 14. DSC patterns of the PP/CPP/MWNT-U composites. [Color figure can be viewed in the online issue, which is available at wileyonlinelibrary.com.]

CONCLUSIONS

In this study, industrial-grade MWNT is used as a conductive filler to prepare PP/CPP/MWNT composites with a MWNT masterbatch obtained through solution processing under ultrasonic irradiation. When compared with the PP/CPP/MWNT composites prepared without ultrasonic irradiation, ultrasonic irradiation is shown to remarkably decrease the volume resistivity of the PP/CPP/MWNT composites. The SEM and TEM results show that ultrasonic irradiation is beneficial to the dispersion of MWNTs in the PP/CPP/MWNT composites and facilitates the exfoliation of the MWNT agglomerates. When the MWNT content exceeds 3.0%, the effect of ultrasonic irradiation on the crystallinity index is obvious. The introduction of ultrasonic irradiation increases the G', G'', and η^* of the PP/CPP/MWNT composites at low frequency. Ultrasonic irradiation improves the interfacial adhesion of MWNTs and the interaction between PP matrix and MWNTs.

Table V. The Crystallinity of PP in PP/CPP/MWNT Composites

Sample code	MWNT (%)	PP (%)	X_C (%)
PP/CPP/MWNT-N 0.5	0.5	97.5	56.9
PP/CPP/MWNT-N 1.0	1.0	95.0	56.8
PP/CPP/MWNT-N 2.0	2.0	90.0	57.4
PP/CPP/MWNT-N 3.0	3.0	85.0	58.4
PP/CPP/MWNT-N 5.0	5.0	75.0	59.5
PP/CPP/MWNT-U 0.5	0.5	97.5	56.5
PP/CPP/MWNT-U 1.0	1.0	95.0	56.3
PP/CPP/MWNT-U 2.0	2.0	90.0	58.1
PP/CPP/MWNT-U 3.0	3.0	85.0	61.2
PP/CPP/MWNT-U 5.0	5.0	75.0	65.1

ACKNOWLEDGMENTS

This work was supported by the National Basic Research Program of China (2005CB623800) and the Young Teachers' Scientific Research Foundation Project of Sichuan University (2012 SCU11024 and 2011SCU11006).

REFERENCES

1. Thostenson, E. T.; Ren, Z.; Chou, T. *Compos. Sci. Technol.* **2001,** *61*, 1899.
2. Chen, G. Z.; Shaffer, M. S. P.; Coleby, D. *Adv. Mater.* **2000,** *12*, 522.
3. Ago, H.; Petritsch, K.; Shaffer, M. S. P. *Adv. Mater.* **1999,** *11*, 1281.
4. Shaffer, M. S. P.; Windle, A. H. *Adv. Mater.* **1999,** *11*, 937.
5. Valentini, L.; Biagiotti, J.; Kenny, J. M. *J. Appl. Polym. Sci.* **2003,** *89*, 2657.
6. Lefenfeld, M.; Blanchet, G.; Rogers, J. A. *Adv. Mater.* **2003,** *15*, 1188.
7. Geng, H.; Rosen, R.; Zheng, B. *Adv. Mater.* **2002,** *14*, 1387.
8. Jin, Z.; Pramoda, K. P.; Xu, G.; Goh, S. H. *Chem. Phys. Lett.* **2001,** *337*, 43.
9. Cadek, M.; Coleman, J. N.; Barron, V.; Hedicke, K.; Blau, W. *J. Appl. Phys. Lett.* **2002,** *81*, 5123.
10. Jia, Z. J.; Wang, Z. Y.; Xu, C. L.; Liang, J.; Wei, B. Q.; Zhu, S. W. *Mater. Sci. Eng. A* **1999,** *271*, 395.
11. Jin, Z. X.; Goh, S. H.; Xu, G. Q.; Park, Y. W. *Synth. Met.* **2003,** *135*, 735.
12. Tang, W. Z.; Santare, M. H.; Advani, S. G. *Carbon* **2003,** *41*, 2779.
13. Paiva, M. C.; Zhou, B.; Fernando, K. A. S.; Lin, Y.; Kennedy, J. M.; Sun, Y. P. *Carbon* **2004,** *42*, 2849.
14. Velasco-Santos, C.; Martinez-Hernandez, A. L.; Fisher, F. T.; Ruoff, R.; Castano, V. M. *Chem. Mater.* **2003,** *15*, 4470.
15. Liang, G. D.; Tjong, S. C. *Mater. Chem. Phys.* **2006,** *100*, 132.
16. Kymakis, E.; Amaratunga, G. A. J. *J. Appl. Polym. Sci.* **2006,** *99*, 84302.
17. Sundaray, B.; Subramanian, V.; Natarajan, T. S.; Krishnamurthy, K. *Appl. Phys. Lett.* **2006,** *88*, 143.
18. Lee, S. H.; Cho, E. N.; Jeon, S. H.; Youn, J. R. *Carbon* **2007,** *45*, 2810.
19. Viswanathan, G.; Chakrapani, N.; Yang, H. *J. Am. Chem. Soc.* **2003,** *125*, 9258.
20. Kang, Y.; Taton, T. A. *J. Am. Chem. Soc.* **2003,** *125*, 5650.
21. McIntosh, D.; Khabashesku, V. N.; Barrera, E. V. *Chem. Mater.* **2006,** *18*, 4561.
22. McIntosh, D.; Khabashesku, V. N.; Barrera, E. V. *J. Phys. Chem. C* **2007,** *111*, 1592.
23. Zhou, Z.; Wang, S.; Lu, L.; Zhang, Y.; Zhang, Y. *J. Polym. Sci. Part B: Polym. Phys.* **2007,** *45*, 1616.
24. Causin, V.; Yang, B. X.; Marega, C.; Goh, S. H.; Marigo, A. J. *Nanosci. Nanotechnol.* **2008,** *8*, 1790.
25. Causin, V.; Yang, B. X.; Marega, C.; Goh, S. H.; Marigo, A. *Eur. Polym. J.* **2009,** *45*, 2155.
26. Vaisman, L.; Marom, G.; Wagner, H. D. *Adv. Funct. Mater.* **2006,** *16*, 357.
27. Lopez Manchado, M. A.; Valentini, L.; Biagiotti, J.; Kenny, J. M. *Carbon* **2005,** *43*, 1499.
28. Xiao, Y.; Zhang, X.; Cao, W.; Wang, K.; Tan, H.; Zhang, Q. *J. Appl. Polym. Sci.* **2007,** *104*, 1880.
29. Donglu, S.; Jie, L.; Peng, H.; Wang, L. M.; Feng, X.; Ling, Y. *Appl. Phys. Lett.* **2003,** *83*, 5301.
30. Xia, H. S.; Qiu, G. H.; Wang, Q. *J. Appl. Polym. Sci.* **2006,** *100*, 3123.
31. Zou, Y. B.; Feng, Y. C.; Wang, L.; Liu, X. B. *Carbon* **2004,** *42*, 271.
32. Safadi, B.; Andrews, R.; Grulke, E. A. *J. Appl. Polym. Sci.* **2002,** *84*, 2660.
33. Garg, A.; Sinnott, S. B. *Chem. Phys. Lett.* **1998,** *295*, 273.
34. Msaon, T. J.; Lorimer, J. P. Sonochemistry: Theory, Applications and Uses of Ultrasound in Chemistry; Ellis Horwood: Chichester, UK, **1988.**
35. Suslick, K. S. *Science* **1990,** *3*, 1439.
36. Yang, L.; Chen, J. Y.; Li, H. L. *J. Appl. Polym. Sci.* **2009,** *111*, 988.
37. Fryczkowski, R.; Slusarczyk, C.; Fabia, J. *Synth. Met.* **2006,** *156*, 310.
38. Yang, L.; Chen, J. Y.; Li, H. L. *Polym. Eng. Sci.* **2009,** *49*, 462.
39. Martin, O.; Roman, C.; Karel, S. *Macromol. Rapid Commun* **2005,** *26*, 1253.